This article is a post-print copy of M. Thunga, K. Larson, W. Lio, T. Weerasekera, M. Akinc, M. R. Kessler. Low Viscosity Cyanate Ester Resin for the Injection Repair of Hole-edge Delaminations in Bismaleimide/Carbon Fiber Composites, *Composites Part A: Applied Science and Manufacturing*, 2013, 52, 31-37. doi:10.1016/j.compositesa.2013.05.001.

Low viscosity cyanate ester resin for the injection repair of hole-edge delaminations in bismaleimide/carbon fiber composites

Mahendra Thunga,
Kelsey Larson,
Wilber Lio,
Thilina Weerasekera,
Mufit Akinc,
Michael R. Kessler

Department of Materials Science and Engineering and Ames Laboratory, Iowa State University, Ames, IA 50011, United States

Abstract

The repair efficiency of bisphenol E cyanate ester (BECy) resin was investigated for the injection repair of high temperature polymer–matrix composites by ultrasonic C-scan mapping, fluorescent dye penetration, optical microscopy, hole plate shear (HPS), and post delamination compression tests. Bismaleimide/carbon fiber (BMI–cf) composites were chosen as a model substrate. A vacuum-based resin injection repair method was used for repairing the pre-damaged composite specimens. The effect of surface wettability on the repair efficiency of BECy on BMI–cf composite substrate was studied by temperature dependent contact angle measurements. C-scan, fluorescent dye penetration, and optical microscopy images of pristine, delaminated, and repaired specimens reveal efficient infiltration of resin in specimens repaired at elevated temperatures. The repair efficiency calculated from HPS and post delamination compression tests was observed to be 155% and 100%, respectively, illustrating the capability of BECy for repairing high temperature structural composites.

Keywords

- Polymer–matrix composites;
- Thermoset resin;
- Mechanical properties;
- Delamination;
- Composite repair

1. Introduction

Polymer matrix composites are gradually replacing the metal alloys in advanced structural applications owing to their high specific stiffness and strength. Polymer matrix composites are typically multi-layer materials consisting of continuous fiber reinforcements embedded in a rigid polymer matrix, resulting in excellent in-plane properties. A major disadvantage of this laminate structure is its high susceptibility to defects and damage in the form of interlaminar fracture, or delamination. This damage can greatly compromise the structural integrity of the material [1], [2], [3], [4] and [5]. Delamination damage is frequently encountered in composites as a result of low energy impact and cyclic thermo-mechanical loading. Patch and scarf repairs are common practices for repairing damaged parts. Although these repair techniques avoid dismantling the damaged structure by applying a reinforcing patch, either bonded or bolted to the composite structure, their applicability is hindered due to limited access to the damage area and the potential for additional damage accrued during the process of removal of the original material. With the growing demand for polymer matrix composites, new repair methods must be developed to overcome the limitations in conventional repair methods. Alternatively, the delamination may be repaired by injecting resin via an access hole into the failed area. This eliminates the need to remove the outer undamaged plies and may result in higher repair strength, provided the adhesive strength of the injected resin is adequate.

In the aerospace industry, high temperature composites are increasingly used for engine cowlings, thrust reversers, and for structural skins subjected to supersonic flows [6]. Next generation airframes, however, are incorporating an increasing amount of bismaelimide based composite structure due to its enhanced, high service temperature capability and increased strength. Determining suitable repair resins for these composite material systems is an active area of development. In order to repair such advanced composites by an injection repair method, the injecting resin must meet the thermo-mechanical properties of the composite. Russell and Bowers [7] identified the following requirements for successful repair: (1) the repair resin should have a cure temperature comparable to the service temperature of the composite material, (2) the resin should cure without releasing volatiles, and (3) the fracture toughness and crack growth resistance within the re-bonded interfaces should be similar to that of the pristine material. The glass transition temperature (T_g) of the cured resin used to repair high temperature panels is critical for a successful repair. The mechanical strength of the repaired structure will decrease significantly when the service temperature of the composite exceeds the T_g of the adhesive. Therefore, the T_g of the cured resin should be significantly above the operational temperature to avoid potential degradation in strength near the service temperature. The flow capability, which depends on the viscosity and surface energy of the resin and substrate, is also a major factor that determines the extent of resin infiltration into the microcracks caused by delamination.

Recently, we have reported that bisphenol E cyanate ester (BECy) is suitable for injection repair of delaminated bismaleimide–carbon fiber (BMI–cf) composites owing to its intrinsic properties, such as low viscosity at room temperature, high thermal stability after cure, high delamination strength, and high fracture toughness on BMI–cf substrates at temperatures as high as 200 °C [8]. The present work focuses on the resin infiltration into composite delaminations and on the effectiveness in restoring the strength of damaged BMI–cf composite parts. The delamination damage was created by a hole plate shear (HPS) technique where a static out-of-plane compressive load is applied to a central hole drilled in the center of the composite panels. Specifically, the success of the resin infiltration was investigated comprehensively by observing in-plane and cross-section views of repaired composite specimens using C-scan imaging, optical microscopy, and fluorescent dye penetration techniques. The mechanical efficiency of the repaired composite specimens was evaluated by studying the in-plane compressive strength and interlaminar shear strength using HPS and post delamination compression tests respectively.

2. Experimental

2.1. Materials

The adhesive resin, bisphenol E cyanate ester (BECy) monomer, is a commercially available resin from Bryte Technologies (Morgan Hill, CA) with product number EX-1510, and was used as received without further purification. The liquid phase organometallic-based polymerization catalyst (EX-1510-B, Bryte Technologies) was supplied with the resin and was used at the manufacturer's suggested loading of three parts per hundred parts resin (phr).

Bismaleimide–carbon fiber (BMI–cf) prepreg was supplied as HTM 512-2 prepreg by Advanced Composites Group, Inc. (Tulsa, OK). The version of the HTM 512-2 prepreg constitutes of balanced 2 × 2 twill weave with 12 K high strength carbon of 660 g/m^2.

2.2. Composite panel manufacturing

The composite panels were manufactured according to specific test requirements. Nine layers of the prepreg were hand-laid at ±45° orientation to achieve a thickness of 0.25 in in the final composite plate. The prepreg plies were cured in an auto-series hot press from Carver. Inc. IA, USA. The panels were processed at 190 °C under 0.6 MPa (90 psi) pressure for 6 h, followed by a free-standing post-cure for 8 h at 240 °C based on a schedule suggested by the supplier.

Square plates 10.16 × 10.16 cm (4 × 4 in.) were machined from the 25.4 × 25.4 cm (10 × 10 in.) plate and a 0.63 cm (0.25 in.) diameter hole with a 82° countersink about one third of the way through was drilled at the center of each plate to facilitate damage initiation and resin injection repair steps. This configuration was chosen based on an early work by Russell and Bowers to represent a typical aerospace fastener hole [7].

2.3. Contact angle measurements

The contact angle measurements were carried out with a ramé-hart 100-00 115 NRL contact angle goniometer, ramé-hart instrument co., NJ. It is equipped with a camera and a video monitor. In order to investigate the wettability of BECy on a BMI–cf composite damaged surface, a 1.27 × 1.27 cm (0.5 × 0.5 in.) delaminated ply taken from a damaged BMI–cf composite panel was used as substrate. The prepared substrate is expected to simulate the delaminated fracture surfaces. The substrate was dried at 150 °C in a convection oven. A temperature controlled sample chamber was used for measuring the temperature dependent contact angle. The temperature dependent contact angle of the BECy resin on five different damaged BMI–cf composite substrate was measured between 30 and 150 °C with an increment of 10 °C step. Due to huge scattering between the contact angles curves measured on different surfaces, only two representative curves were considered for discussion. The contact angles from both left and right sides of the resin drop were measured and averaged. The drop was allowed to equilibrate for 10 min before each measurement.

2.4. Ultrasonic scanning (C-scan)

An air-coupled, through-transmission ultrasonic system with 120 kHz focused probes was used to create C-scans. Prior to scanning, the hole in each plate was filled with putty and the plates were surrounded by a foam frame. Both these techniques were used to minimize the noise around the hole and edges by preventing excess sound leaks. The scans were obtained for the pristine, delaminated, and repaired samples to study the infiltration efficiency of the resin.

2.5. Imaging and quantifying the damage

Pristine, delaminated, and repaired HPS specimens were sectioned diagonally through the center of the hole to image the cross-section by optical microscopy and fluorescent dye penetration measurements, as shown in Fig. 1. The cross section surface was finely polished before microscopic images were collected in reflection mode using Olympus BX51. The fluorescent dye penetration tests were performed by using Zyglo ZL-56 fluorescence dye penetrant [9]. In both optical microscopy and fluorescent dye penetration measurements, the surface images were merged to produce the microscopic image of a 2.56 cm (1-in.) cross-section from the damaged zone. The optical microscopic images were further used to quantify the crack filling capability of BECy resins. The delaminations, microcracks, and air voids in the samples were traced to construct the crack structure. The crack lengths were measured manually, using calipers and then compared between the investigated specimens.

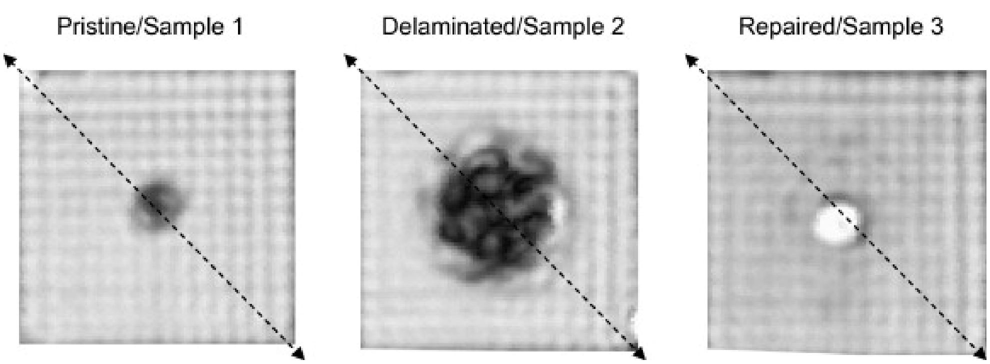

Fig. 1: C-scan images of pristine, delaminated, and repaired specimens used for fluorescent dye penetration and optical microscopy investigations.

2.6. Hole plate shear (HPS) method

The sample geometry and test setup for HPS technique is shown in Fig. 2. The HPS specimen was secured between two steel plates (both with a 5.08 cm (2-in.) diameter circular hole in the center) that act as a clamp and centered under the load cell. A steel ball bearing was placed on the countersink hole where the load was applied. Each sample experienced an initial static load of 250 N, followed by a compressive load applied at a rate of 1 mm/min (0.039 in/mm) until a 2-mm (0.078 in.) extension was reached. The repair efficiency was calculated by averaging the load baring capacity of at least 5 HPS samples from pristine, delaminated and repaired specimens.

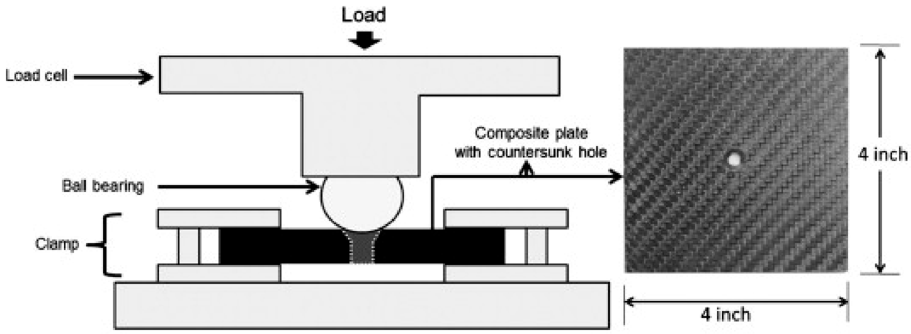

Fig. 2: The hole plate shear (HPS) test setup. HPS specimen is shown on the right.

2.7. Post delamination compression test

Pristine, delaminated, and repaired HPS specimens were modified into double-edge-notched tension (DENT) specimens for compression-after-HPS tests as shown in Fig. 3. The specimens were machined into 10.16 × 5.08 (4 × 2-in.) plates with v-notches on either sides of the plate in-line with the center of the center hole. A standard (ASTM Standard D 7137) CAI test fixture was modified to accommodate DENT specimens. The fixture and specimen were loaded onto a 50 kN Instron 5569 tensile testing machine (Norwood, MA) at a compressive extension rate of 1 mm/min until a sudden drop in the load–displacement curve was recorded. Data from five specimens that failed through the repair region and center hole were included in the calculations. The failure load is obtained from the maximum load in load–displacement curves. The post delamination compression strength (σ_c) was calculated using the following equation:

$$\sigma = \frac{F_{\max}}{b.t}$$

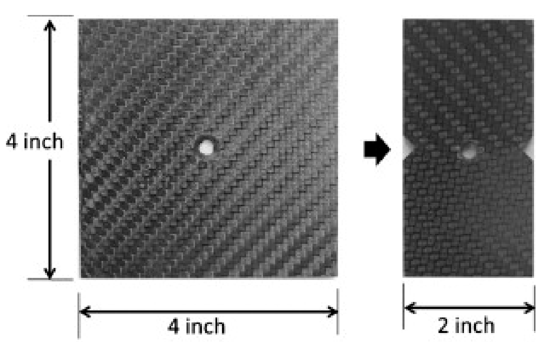

Fig. 3: Specimen modification for compression after impact test (CAI). Notches were added on both sides of the HPS specimen to prepare specimens similar like DENT specimen for post delamination compression tests.

where $F_{\max}$ is the failure load, b is the width of the specimen between notches after subtracting the hole diameter, and t is the thickness of the specimen.

2.8. Injection repair setup

Based on the resin-injection repair methods developed by Russell et al. [3] and [10] and Dehm et al. [11], a prototype vacuum-assisted repair set-up was designed to achieve efficient infiltration of resin into the delamination areas (Fig. 4). In this setup, the vacuum pump and resin injection syringe are attached to the same access hole. In our recent communication [8] we reported that the moisture in the BMI–cf composite substrates showed adverse effects on the bond strength between BECy and the BMI–cf substrate. Thus, the damaged specimens were pre-dried at 120 °C for 8 h in a vacuum oven. The repair was conducted both at room temperature and at 100 °C to study the influence of repair temperature on resin infiltration. For high temperature repairs, the whole setup was placed in a convection oven at 100 °C. After injecting the resin, the specimen was placed in the oven again to fully cure the injected resin at 180 °C for 2 h, followed by a post-cure at 250 °C for 2 h, at a heating rate of 1 °C/min. Before further testing, the resin-filled holes were re-drilled.

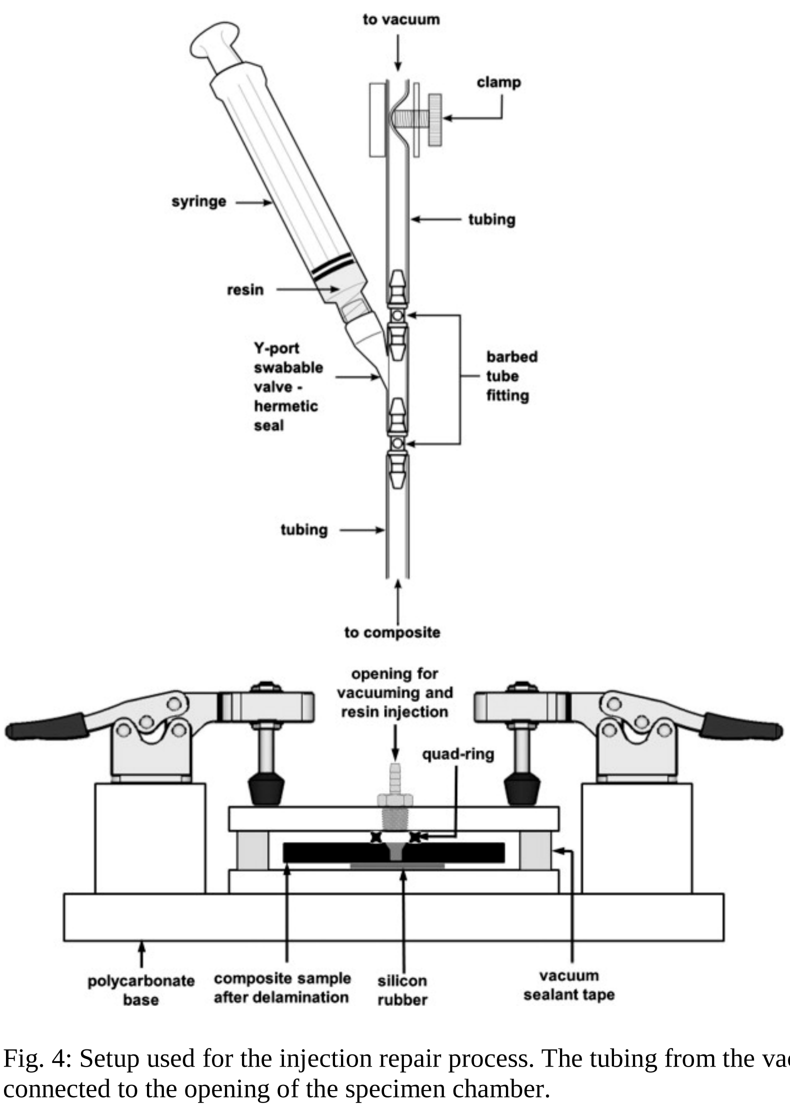

Fig. 4: Setup used for the injection repair process. The tubing from the vacuum pump and resin syringe are connected to the opening of the specimen chamber.

3. Results and discussion

3.1. Contact angle measurements

The temperature dependent contact angle of BECy resin was measured on the BMI–cf substrate to determine the wettability of the resin needed for effective infiltration of BECy into the composite delamination areas. Fig. 5 illustrates the influence of temperature on the contact angle of BECy on a BMI–cf composite substrate. The contact angle was measured with different BECy drop volumes on two different BMI–cf composite substrates. The variation in the contact angle between curves 1 and 2 in Fig. 5 could be caused by the difference in the nature of the surface roughness and drop volume. The contact angles on both substrates appear to be stable between 40 and 90 °C. However, the contact angle starts to gradually decrease at approx. 90 °C. The decrease in contact angle may be attributed to either a decrease in the surface tension of the BECy resin or an increase in the surface energy of the composite substrate. The error in contact angle at individual temperature steps is negligible. Based on the contact angle measurements and upper temperature limits of the experimental set up, the temperature was set at 100 °C for all repair experiments.

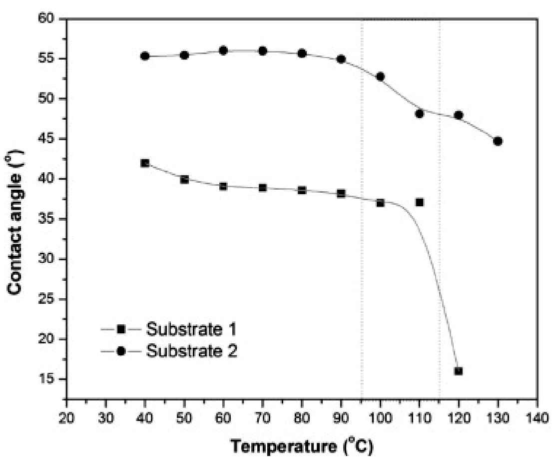

Fig. 5: Influence of temperature on the contact angle of BECy on BMI–cf substrate. The characteristic temperature range desired for repair is indicated between the dotted lines.

3.2. Ultrasonic scanning (C-scan).

An air-coupled ultrasonic imaging technique (C-scan) was used to observe the effectiveness of BECy infiltration after injection. Close examination of the damaged specimens confirm that the HPS is successful in introducing controlled and reproducible delamination in the specimens. To confirm the effect of temperature on the repair effectiveness, the C-scan images of specimens repaired both at room temperature and at 100 °C were obtained and are illustrated in Fig. 6. The images of repaired specimens illustrate that the infiltration of BECy into the damage zone was successful for the specimens repaired at 100 °C, whereas only partial infiltration was observed for specimens repaired at room temperature.

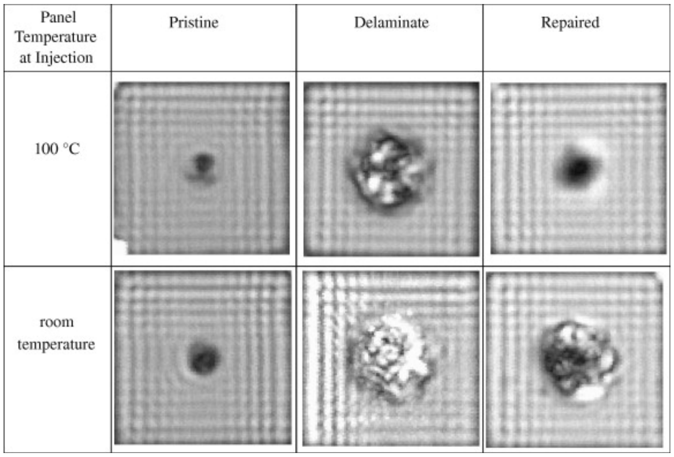

Fig. 6: C-scan images of pristine, delaminated, and repaired specimens repaired at room temperature and at 100 °C.

3.3. Imaging and quantifying the damage

To further illustrate the degree of BECy infiltration into the delaminated area, a fluorescent dye penetration test was performed. The specimens were sectioned diagonally and examined via optical microscope under ultraviolet light at 5× magnification, causing the fluorescent dye to glow and clearly display the delamination areas within the samples. The C-scan images of specimens selected from pristine, delaminated, and high temperature repaired samples used for fluorescent dye penetration tests were shown in Fig. 1. The cross sections of the fluorescent dye penetration microscopy images for pristine, delaminated, and repaired specimens are shown in Fig. 7. The presence of short cracks on the pristine surface is caused by the pre-existing air voids formed during the composite manufacturing process. In the damaged specimen, traces of fine fragment cracks as a result of delamination in the composites are evident. Interestingly, the cracks are completely absent in the repaired specimens. This qualitatively confirms the successful infiltration of resin as observed in the C-scan images.

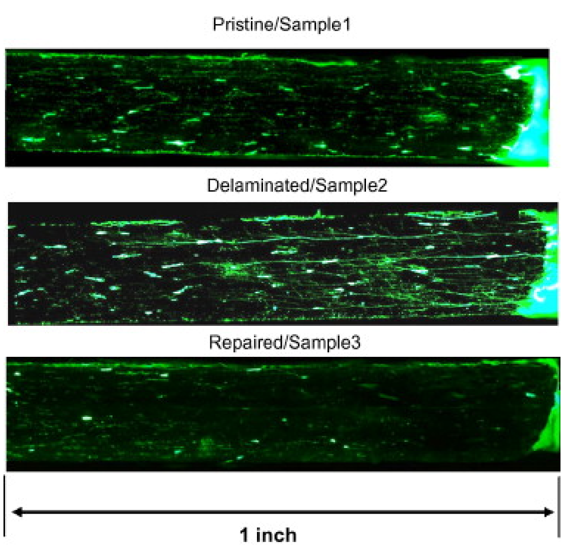

Fig. 7: Microscopy images of fluorescent dye on the transverse cross-section surface of pristine, delaminated, and repaired BMI–cf specimens.

The crack paths in the pristine, delaminated, and repaired samples were traced using Adobe Photoshop CS4 to map out a skeleton of the cracks. The optical microscopic images along with the traces of cracks are shown in Fig. 8. While the C-scans and fluorescent dye penetration tests confirmed successful resin-infiltration into the microscopic cracks, the quality of the bond was evaluated by comparing the mechanical properties of pristine, delaminated, and repaired specimens. HPS and Post delamination compression techniques were used to determine the mechanical strength that was restored after repair.

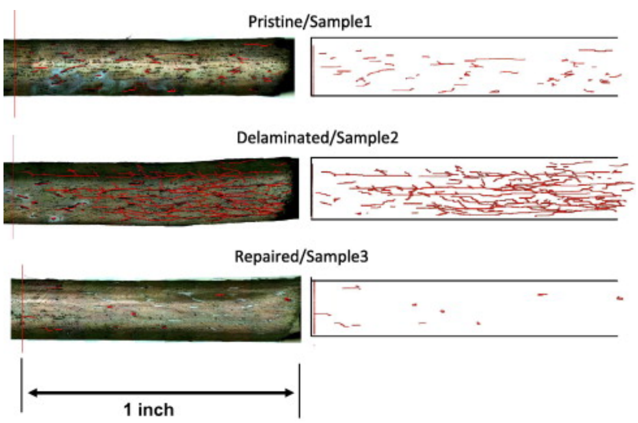

Fig. 8: Microscopy images of the transverse cross-section view of BMI–cf specimens with traces of cracks on the left side and a skeletonization of the crack lengths on the right side.

3.4. Hole plate shear (HPS) test

In order to study the interlaminar shear strength restored after repair, the load bearing capacity of the pristine, delaminated, and repaired HPS specimens were measured in HPS mode. Fig. 9a depicts the load–compressive extension curves of the investigated specimens. The curves for pristine and repaired specimens exhibit a peak load, followed by load instability. The peak load behavior is caused by the initiation of cracks in the specimen after a critical load is reached. The load instability after crack initiation corresponds to interlaminar stick-slip type crack propagation. The average peak loads of the samples are summarized in Fig. 9b. The peak load and the load point displacement at crack initiation for repaired specimens are higher than those of pristine specimens because the voids originally present in the composite were also filled with the BECy, as illustrated in Fig. 7 and Fig. 8. However, in delaminated specimens, the absence of such bonding resulted in weak load-bearing capacities, as observed in Figs. 9a and b. From the average peak load values, the efficiency of repair was calculated using the following equation:

$$E_R = \left[\frac{F^R - F^D}{F^P - F^D}\right]$$

where E_R is the repair efficiency, F^R, F^D, and F^P are the peak loads for the repaired, delaminated, and pristine specimens, respectively. Because the delaminated specimens did not show a distinct peak in the load–extension curves, the peak load for the delaminated specimens was assigned as the load value at the same extension for the maximum load observed for pristine specimens. The repair efficiency was estimated to be 155%, demonstrating the superior strength of the BECy repaired sample compared to the strength of the pristine sample. Russel et al. [12] reported a maximum repair efficiency of 92% in resin infiltrated specimens for the repair of graphite/epoxy aircraft polymer matrix composites via the HPS method. The higher repair efficiency for BECy compared to the epoxy resin may be owing to the increased bond strength between BECy and the BMI–cf polymer matrix composites compared to the bond strength between epoxy and the graphite/epoxy composites.

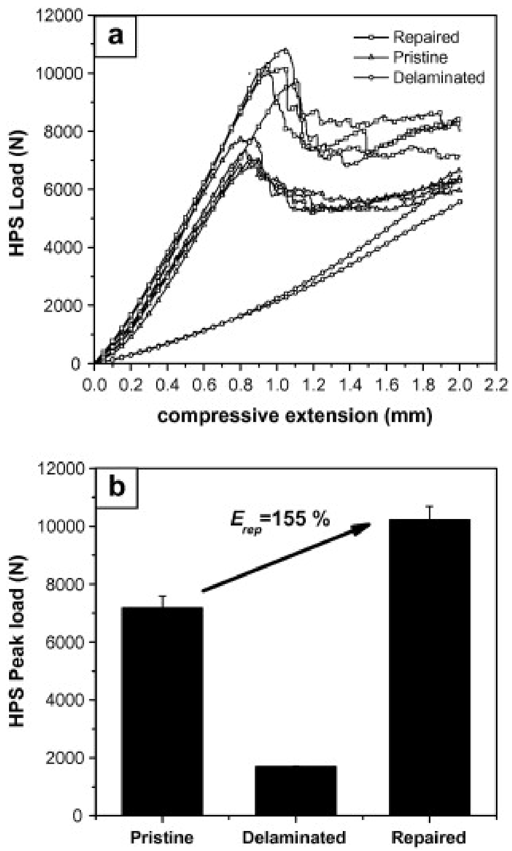

Fig. 9: HPS testing of pristine, delaminated, and repaired specimens. (a) Load–compressive extension curves for the investigated HPS specimens. (b) Maximum HPS load from load–compressive extension curves.

3.5. Post delamination compression tests

Compression after impact test is widely used to measure the residual compressive strengths of composites after impact loading [13]. However, in the present work, the same technique is used on specimens damaged via the HPS method instead of impact loading. The undamaged section of the HPS specimen was removed to localize the applied stress at the damage zone (Fig. 2). This sample modification was intended to force buckling at the repaired zone. The compressive stress required for localized buckling of pristine, delaminated, and repaired specimens is an indication of their in-plane compressive strength. The post delamination compression test setup and the test results are shown in Fig. 10a and b, respectively. A significant drop in post delamination compression stress from 275 MPa to 125 MPa was observed in the delaminated specimens when compared to pristine specimens. However, in repaired specimens, the post delamination compression stress was completely restored to that of pristine specimens, revealing 100% repair efficiency after a repair using BECy. The formation of a strong bond between the delaminated cracks in the repaired specimen is believed to facilitate the complete recovery of the strength in the through-thickness direction.

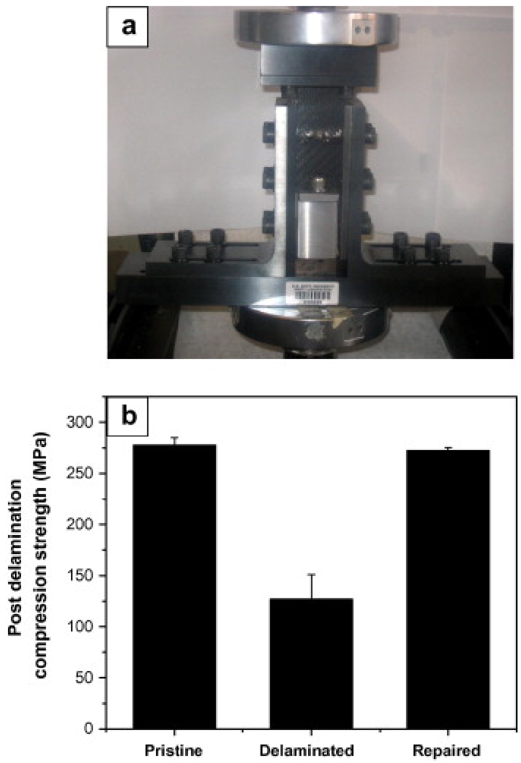

Fig. 10: Post delamination compression stress of pristine, delaminated, and repaired specimens. (a) Experimental setup for post delamination compression tests with double-edge-notched-tensile (DENT) specimen. (b) Maximum post delamination compression stress of pristine, delaminated, and repaired specimens.

4. Conclusion

Damage in BMI–cf polymer matrix composites was successfully repaired by injecting BECy resin using a vacuum-based repair setup at 100 °C. Repair temperature was observed to be a key factor for obtaining successful infiltration of resin into the delamination areas of damaged specimens. Qualitative evaluation of repair efficiency from ultrasonic C-scan imaging, fluorescent dye penetration tests, and optical microscopy revealed complete infiltration of BECy resin into the delaminated areas. Furthermore, a repair efficiency of 155% in HPS test and 100% in post delamination compression test demonstrates the ability of BECy to restore the structural strength of BMI–cf composites. Therefore, BECy was observed to be an excellent resin for repairing BMI–cf composite panels that are commonly used for high temperature applications. The HPS method employed in the current work provided a central hole for infiltration of the repair resin. To repair impact induced delaminations, a hole would need to be drilled into the damaged laminate to allow access for the resin to be injected to the delamination. This is a topic of current work in our group.

Acknowledgements

Authors gratefully acknowledge the financial support from "Strategic Environmental Research and Development Program (SERDP)," (Project Number WP-1580). Special thanks to Dr. Vinay Dayal (Department of Aerospace Engineering, Iowa State University) for helping with CAI tests and Dan Barnard (Center for Nondestructive Evaluation, Iowa State University) for guidance in C-Scan imaging and providing access to their laboratory facilities.

References

[1] G.B. McKenna. Interlaminar effects in fiber-reinforced plastics-a review. Polymer-Plast Technol Eng, 5 (1975), pp. 23–53.

[2] K.W. Wu, C.L. Lee, Y.C. Chang, C.L. Ong. Compressive strength of delaminated and repaired composite plates. Mater Chem Phys, 43 (1996), pp. 173–177.

[3] A.J. Russell, J.S. Ferguson. Composite repair issues on the CF-18 aircraft. Rep. no. AGARD-CP-550-PAP-14. Defense research establishment Pacific, Victoria BC (CAN) (1995) .

[4] A.A. Baker. D.H. Middleton (Ed.), Composites materials in aircraft structures, Addison-Wesley Longman, Limited, New York, England (1990), pp. 207–227.

[5] W.J. Cantwell, J. Morton. The significance of damage and defects and their detection in composite materials: a review. J Strain Anal Eng, 27 (1992), pp. 29–42.

[6] E. Ahci, R. Talreja. Characterization of viscoelasticity and damage in high temperature polymer matrix composites. Compos Sci Technol, 66 (2006), pp. 2506–2519.

[7] Russell AJ, Bowers CP. Resin requirements for successful repair of delaminations. In: Proceedings of the 36th international SAMPE symposium, vol. 36; 1991. p. 2279–290.

[8] M. Thunga, Y.L. Wilber, M. Akinc, M.R. Kessler. Adhesive repair of bismaleimide/carbon fiber composites with bisphenol E cyanate ester. Compos Sci Technol, 71 (2011), pp. 239–245.

[9] T. Kuboki, T. Hilvo, P.Y.B. Jar. Detection of interlaminar cracks in fiber-reinforced polymers. J Mater Sci Lett, 21 (22) (2002), pp. 1789–1791.

[10] A.J. Russell, C.P. Bowers. Repairing delaminations with low viscosity epoxy resin AGARD-CP-530-PAP-25. Defense Research Establishment Pacific, Victoria BC (CAN) (1992) .

[11] S. Dehm, D. Wurzel. Fast in-situ repair of aircraft panel components. J Aircraft, 26.5 (1989), pp. 476–481.

[12] A.J. Russell, C.P. Bowers, A.J. Moss. Repair of delamination and impact damage in composite aircraft structures. Proceedings of the 6th international conference on composite structures, Barking, England: Elsevier Science Publ. Ltd., Paisley, Scotl (1991), pp. 145–159.

[13] M.D. Freitas, L. Reis. Failure mechanism on composite specimens subjected to compression after impact. Compos Struct, 42 (4) (1998), pp. 365–373.